ESR Study of the Spin Adducts of three analogues of DEPMPO substituted at C₄ or C₃

Florence Chalier, [a]* Jean-Louis Clément,[a] Micaël Hardy,[a] Paul Tordo,[a] and Antal Rockenbauer [b]

before proofs

In the research program of some new derivatives of spin-trap DEPMPO (5-diethoxyphosphoryl-5-methyl-1-pyrroline-*N*-oxide) leading to various radical adducts with photogenic ESR signals, three various phosphorylated pyrroline-N-oxide were studied in spin trapping. These nitrones were proved to trap a variety of free radicals to afford adducts presenting characteristic ESR signals enabling unambiguous identification of the radical species trapped. From the general patterns of the signals, the adduct geometries were determined. Two of nitrones bore a hydroxylmethyl substituent (HM) on the pyrroline ring, either at C₃ or at C₄. The two diastereoisomers of nitrone 4-HMDEPMPO, whose synthesis has been already described, were separately studied. The isomer (4R*, 5R*) of 4-HMDEPMPO afforded stereoselectively, with superoxide or peroxyle radicals, *trans* adducts *versus* phosphoryl group, however, formed of two rotamer sets in chemical exchange. In comparison with DEPMPO adducts, the exchanges rates of the conformer sets of 4-HM$_{cis}$DEPMPO-OOH and 4-HM$_{cis}$DEPMPO-OO^{t}Bu were 9-fold or 2-fold smaller respectively. The eight line signals of theses adducts were easily recognisable. The trapping of the same radicals with the other diastereoisomer (4S*, 5R*)-4-HMDEPMPO or with (3S*, 5R*)-3-HMDEPMPO, obtained via oxidation of a phosphorylated pyrroline, led to more complicated spectra owing the formation of diastereo-isomer adducts. The signal of each diastereoisomer adduct was simulated with two species in conformational exchange. In comparison with DEPMPO, the *cis*-C₄-substitution was proved to slow down 26-fold the exchange rate between the two rotamer sets of the *trans* superoxide-adduct versus phosphoryl group. The *trans*-C₃-substitution was proved to slow down 18-fold, at 223°K, the exchange rate between the two rotamer sets of the *trans* terbutylperoxyl-adduct. The last nitrone, a bicyclic one, named MEOOPPO (6a-methyl-(6-ethoxy-5-oxa-6-oxaphospholan-6-yl)1-pyrroline-*N*-oxide) was obtained directly from (4R*, 5R*)-4-HMDEPMPO in basic conditions. Superoxide with the rigid MEOOPPO reacts exclusively in *trans* addition *versus* phosphoryl group, however, the adduct obtained in aqueous buffer was not very persistent and the nitrone was partially degraded during 30 min storage. For every nitrones, the hydroxyl radical was not added stereoselectively on one ring face and some diasteroisomer adducts were obtained.

Introduction

Nitrones have been used to trap various oxygen centred radicals. However, with the superoxide, O₂⁻•, which is the

[a] *Laboratoire SREP, Institut de Chimie Radicalaire - UMR 7273, CNRS and Aix-Marseille Univ. - case 521, Centre de Saint Jérôme, 13397 Marseille Cedex 20, France.*
b *Research Centre for Natural Sciences, Institute for Molecular Pharmacology, H-1525 Budapest, PO Box 17, Hungary.*
* *To whom correspondence should be addressed. Dr F. Chalier, Phone 33 4 91 28 89 23; Fax 33 4 91 28 87 58; e-mail: florence.chalier@amu.univ-mrs.fr*

primary upstream radical of the radical reaction chain of the oxidative stress [1] and is induced in several physiological disorders, the nitrone adducts were generally too short-living. With the very popular nitrone DMPO,[2] the half-life time of the superoxide adduct is inferior to 1 min. The trapping of the hydroxyl radical, HO•, which is the predominant species contributing to cellular damages, afford adducts more persistent. Compared with DMPO, the phosphorylated nitrone DEPMPO[3] (Scheme 1) presents three major advantages. The first marked advantage is the higher persistency of its adducts with the oxygen centred radicals. For example the half-life of the superoxide adduct is 15 times higher than that of adduct

DMPO-OOH and the alkylperoxyl radicals adduct can be observed in aqueous phase.[4] The second advantage is that the decomposition of the superoxide adduct into another paramagnetic species since, the hydroxyl adduct was proved not to be spontaneous and can be avoided by using a superoxide concentration inferior or equal to 0.5 mM, as found *in vivo*. The third advantage is the additional information obtained from the phosphorus-coupling constant allowing an easier identification of the trapped radical structure. The ESR spectra of the superoxide adduct (DEPMPO-OOH) and of the peroxyl radical adducts (DEPMPO-OOR) have some characteristic shape signals and were attributed mainly to one diastereoisomer adduct obtained after the *trans* addition of the radicals *versus* the phosphoryl group, on the less hindered face of the pyrroline ring. However, each signal exhibited a dramatic alternating linewidth owing to a sufficiently slow chemical exchange between two sets of conformers of the diastereoisomer. This phenomenon may impede the accurate identification of the radicals trapped *in vivo* from spectra containing the superimposed signals of several adducts. As the ESR signal patterns of adducts formed is correlated to their geometries, we decided to simplify the spectra obtained through a geometry of the initial nitrones favouring stereoselective formation of adducts and their fast conformational exchange. Introduction of a phenyl group on the ring of DMPO trap induces a rigid conformation of this ring and is therefore beneficial for the superoxide radical trapping.[5] Earlier studies showed that the pseudorotation occurring within the ring of stable β-phosphorylated pyrrolidinyloxyl radicals was slowed down by the ring substitution with a phenyl group.[6] In the DEPMPO series, synthesis of the 3-phenyl[7] and 4-phenyl[8] and 4-hydroxymethyl[9] DEPMPO analogue named 3-PhDEPMPO, 4-PhDEPMPO and 4-HMDEPMPO respectively (Scheme 1), were recently reported.
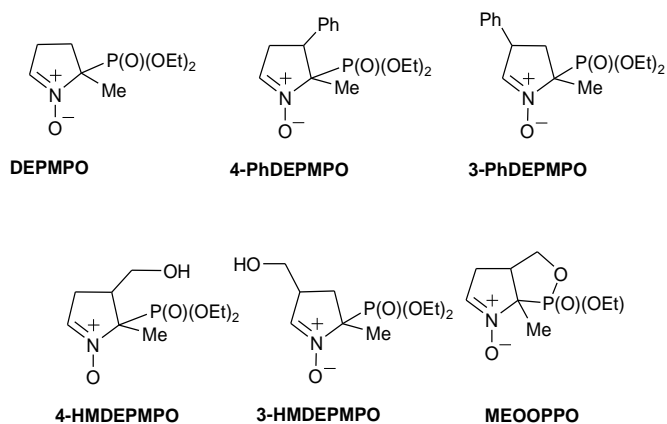
**Scheme 1.** Chemical structures of DEPMPO and new derivatives.

The presence of both kinds of substituents led to an important steric effect on the course of addition of the superoxide radical. In the presence of superoxide, the *cis* diastereoisomers of these three nitrones, where the phosphoryl group and the phenyl or hydroxymethyl substituent are in *cis* position, afforded stereoselectively *trans* adducts. Compared to DEPMPO-OOH,

the superoxide *trans* adduct versus phosphorus on (3R*, 5R*)-3-PhDEPMPO or (4R*, 5R*)-4-PhDEPMPO are respectively less persistent, or at least so persistent when the trans adduct with (4R*, 5R*)-4-HMDEPMPO is more persistent with a 25% longer half-life. Moreover, the signal of these adducts present also the alternating line-width phenomenon due to a slow chemical exchange between two conformer sets, with a rate constant on the same order than that of DEPMPO-OOH. The spin trapping behaviour of the diasteroisomeric forms of this nitrone are described thoroughly hereafter and compared to the spin trapping behaviour of two new substituted DEPMPO derivatives including a C_3-substituted analogue (nitrone 3-HMDEPMPO Scheme 1) and a bicyclical one named MEOOPPO (Scheme 1). We investigate relationship between the substitution of the pyrroline ring and the general patterns of the adduct signals.

Results and discussion

Synthesis of Nitrones 3-HMDEPMPO and MEOOPPO.
The nitrone 3-HMDEPMPO (5-diethoxyphosphoryl-5-methyl-3-hydroxymethyl-1-pyrroline N-oxide) substituted at C_3 was prepared in a two-step synthesis from 4-hydroxymethyl-2-methyl-1-pyrroline **4** that could be issued from an eight-step synthesis[10] or from the four-step synthesis given in Scheme 2. It was obtained by cyclisation of an adequate γ-aminoketone.
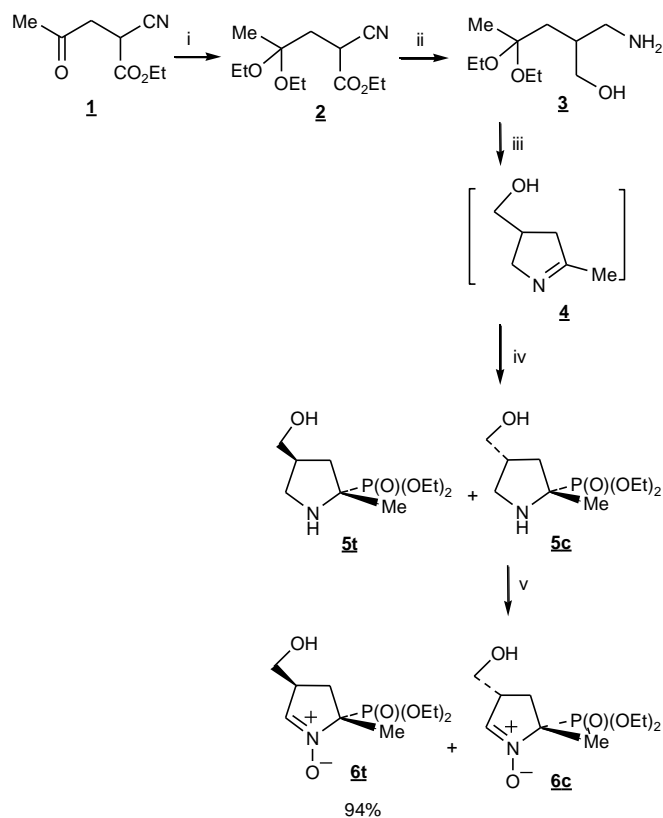
Scheme 2. Synthesis of nitrone 3HMDEPMPO. *Reagents and conditions: (i) HC(OEt)₃, resin Amberlyst 15, CH₂Cl₂, 0-5 °C, 99%; (ii) LiAlH₄, THF, 3h at 25 °C, then 1h at 57 °C, 36%; (iii) 1) HCl THF/H₂O (5:1), rt, 2) K₂CO₃ THF/H₂O (5:1), rt; (iv) HPO(OEt)₂, rt, 40%; (v) H₂O₂, Na₂WO₄, CH₃OH/H₂O (2:1), 4 °C, 32%.*

Synthesis of ethyl 2-cyano-4-diethoxypentanoate **2** is described,[11] but we obtained **2** *via* the quantitative transacetalisation of ethyl 2-cyano-4-oxopentanoate **1**, which was synthesized from chloroacetone and ethyl cyanoethanoate.[12] The yield (36% not optimized) of the reduction step of the cyano and ester functions of **2** using LiAlH$_4$ was lowered by formation of by-products such as some conjugated oxoenamines. The amino function of 2-aminomethyl-4-diethoxypentan-1-ol **3** was let to react with the carbonyl function delivered by HCl to afford the expected 4-hydroxymethyl-1-methyl-2-pyrroline **4**. This pyrroline was not isolated and was let crude to react with diethylphosphite. The ensuing phosphorylated pyrrolidine **5** was obtained in 40% yield with an 94% excess of the (3R*, 5R*) diastereoisomer (**5t**) where the hydroxymethyl substituent and the phosphoryl group are in *trans* position. This pyrrolidine was easily oxidized to nitrone **6** (Scheme 2), under mild conditions using the system (H$_2$O$_2$-sodium tungstate) in aqueous methanol. The two diastereoisomers of nitrone 3-HMDEPMPO **6** were not separated. However, the isomer mixture contained mainly (94%) the (3R*, 5R*) diastereoisomer (**6t**).

The bicyclical nitrone (**8**) called MEOOPPO was actually obtained in 45% yield from the (4R*, 5R*) diastereoisomer of nitrone 4HMDEPMPO[9] (named hereafter **7c**) where the phosphoryl group and the hydroxymethyl substituent are in *cis* position (Scheme 3). The purification of **8** was not straightforward and needed a dry atmosphere because **8** was easily hydrolyzed. This nitrone was degraded in a few weeks in spite of its storage in an inert atmosphere at −18°C.
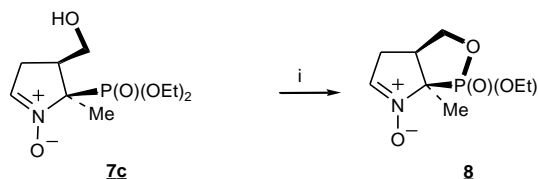
Scheme 3. Synthesis of nitrone MEOOPPO. *Reagents and conditions: (i) NaH, DME, rt, 45%.*

ESR Studies.

In the present work, the spin trapping capacities of the nitrones were tested in aqueous phase mainly toward superoxide and the hydroxyl radical, two oxygen centred radical species that are of the largest biological relevance. Trapping of several carbon centred species was also tested in aqueous buffer and trapping of a bulky peroxyl radical was investigated in organic phase. When ESR signal increased in the first minutes of experiments the spectra recorded and given hereafter corresponded to the largest signals. Assignment of the signals was done through their simulation (gray coloured lines in the figures of the spectra) using the ESR software ROKI developed in the Central Research Institute of Chemistry, Hungary.[13] Four types of hyperfine coupling constant $a_{H\gamma}$ (3 various constants for the H of the ring and one for the 3 H of the methyl substituent), were sometime used in simulation for a better fit even when no superhyperfine structure of the pattern was seen. The two

diasteromeric forms, (4R*, 5R*)-4-HMDEPMPO (**7c**) and (4S*, 5R*)-4-HMDEPMPO (**7t**), led to adducts with different spectra and different coupling features. Therefore, they were distinctively studied. The calculated values of the coupling constants are given in Table 1 for the diastereoisomer **7c**, and in Table 3 for the other diastereoisomer (4R*, 5R*) diastereoisomer of nitrone 4HMDEPMPO[9] **7t** and for the cyclical nitrone MEOOPPO **8**, and in Table 4 for nitrone 3-HMDEPMPO **6**. Because of the preponderance of the *trans* diastereoisomer (**6t**) in the nitrone 3-HMDEPMPO samples, the major signals observed in the spin trapping experiments were assigned to the **6t** adducts.

a) Spin Trapping of Superoxide: superoxide was generated in phosphate buffer at pH 7.3 containing DETAPAC (diethylenetriaminepentaacetic acid) using two systems such as the well-known [xanthine oxidase / oxygen / hypoxanthine system] ([XO / O$_2$ / HX] system) or as the [KO$_2$ / crown ether /DMSO] system. Unambiguous assignment of the signals obtained in the presence of the nitrones to the superoxide adducts was supported by their similarity when using both generating systems and by their complete inhibition when superoxide dismutase (SOD) was added in the [XO / O$_2$ / HX] mixture. The spectra observed in the presence of superoxide were given in Figure 1. Each spectrum of superoxide trapping showed an alternate line-width phenomenon which was attributed, like for DEPMPO-OOH, to a slow exchange between two conformers sets for each diastereoisomer adducts when the two are present. The simulation of the signals was
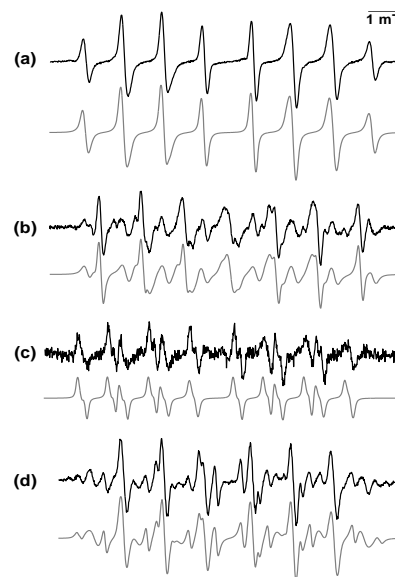

Figure 1. Spin trapping of superoxide with nitrones 7 or 8 or 6. Spectra obtained (dark lines) and computer simulated (gray lines) from a mixture containing HX (0.4 mM), XO (0.04 U mL^{-1}), DETAPAC (1 mM) in phosphate buffer (0.1 M, pH 7.3) in the presence of (a) **7c** (61 mM) after 9 min incubation and argon bubbling (1 min); (b) **7t** (50 mM) after 7 min incubation; (c) **8** (50 mM) after 3 min incubation and 3 scans; (d) **6** (50 mM) after 7 min incubation. *Spectrometers settings: microwave power 10 mW; modulation amplitude, 0.702 (a-b), 0.497 (c), 0.787 (d), 1 (h); time constant, 0.128 s; gain 10^5; sweep time, 83.89 s (a-c), 335,54 s (d); conversion time, 82 ms (a-c), 327.68 ms (d).*
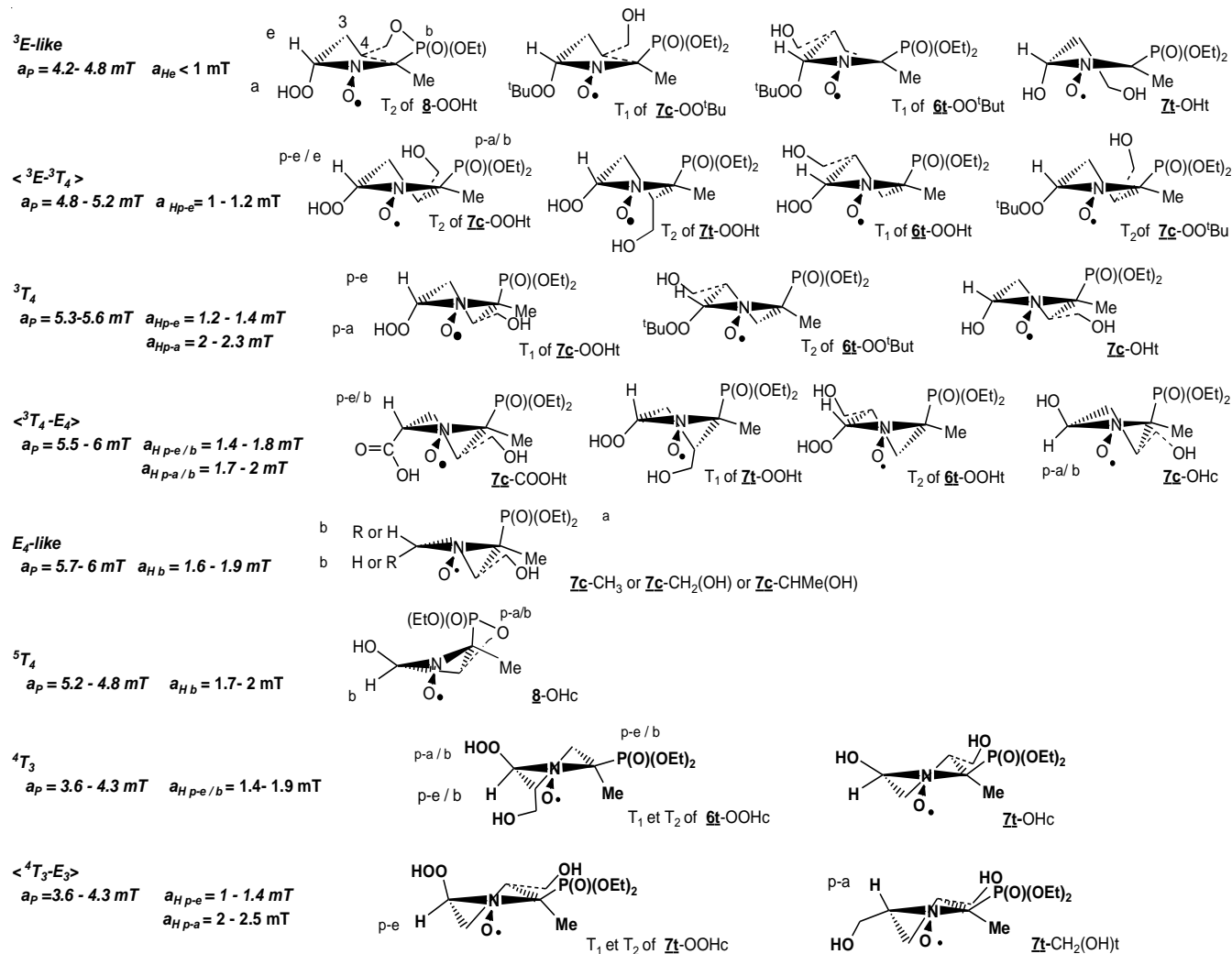
done assuming that only the H_β and ^{31}P couplings differed significantly in the two conformer sets while the g factor, the ^{14}N couplings and the hydrogen γ-hfcs were very close. The relaxation contribution in the hyperfine lines was also considered the same for the two sets. For DEPMPO-OOH, four simulation solutions for the two conformation sets could be found at ambient temperature conditions.[14] These solutions differed by the H_β and ^{31}P coupling values and the populations p_1 et p_2 of the minor and major conformer set. The coupling values averaged on the two sets ($\langle A \rangle = p_1A_1 + p_2A_2$) are the same for all the solutions. These average values induce the lines positions of the signal observed and explain the line width alternation. Decreasing the exchange rate in a lower-temperature domain allowed discriminating the best solution that was the two conformer sets with the largest Ap difference, and the preponderant set had the highest A_P values.

We already reported[9] the ESR parameters of the superoxide adduct with the *cis* diastereoisomer 4-HM$_{cis}$DEPMPO (**7c**) at

the outcome of experiments using the [KO_2 / crown ether] system or ([XO / O_2 / HX] as generating system. The **7c**-OOH signal (given in Fig 1a) quite asymmetric was observed alone in the first minutes of experiments (more than 10 min of incubation with [XO / O_2 / HX] system) has be shown to be due to only one diastereoisomer form (the *trans* adduct **7c**-OOH$_t$ versus phosphorus group) of the superoxide adduct in two conformers sets in a relative slow chemical exchange although one was preponderant. We give again herein theses ESR parameters in Table 1, as well as a second simulation solution to the observed spectrum given in Figure 1a. The second simulation solution presented an equal regression coefficient for a higher A_p difference for the two sets and a higher difference also in their populations. However, the first solution dominated (with the best regression coefficient), in simulation of a series of spectra scanned when the exchange rate between the conformer sets was slowing down by increasing the solvent viscosity.[9] As it was demonstrated by Pople and Cremer, [15] the

Table 1 ESR parameters of several radical adducts with 4-HM*cis*DEPMPO mainly at 298K

Adduct	Adduct generating system	Diastereoisomer (regression coefficient)	Conformers & Exchange rate k (s^{-1})	A_P (mT)	A_N (mT)	$A_{H\beta}$ (mT)	$A_{H\gamma}$ (mT)
7c -OOH	(HX / O_2 / XO) in 0.1 M buffer at 298k	*Trans* from ref [9] (R = 0.9956)	T_1 (62 %) T_2 (38 %) 1.73×10^7	5.442 5.223	1.290 1.315	1.248 1.086	0.010×3 0.054 0.039 0.072 0.010×3 0.054 0.039 0.072
		Or Trans (R = 0.9966)	T_1 (21 %) T_2 (79 %) 3.47×10^7	5.677 5.289	1.257 1.309	1.512 1.116	0.016×3 0.080 0.073 0.041 0.016×3 0.080 0.073 0.041
7c -OOCH$_3$	Fenton reaction / DMSO 5% / O_2 in 0.1 M buffer at 298k	*Trans*	T_1 (72 %) T_2 (28%) 0.98×10^7	5.372 5.020	1.306 1.303	1.145 1.013	0.033×3 0.069 0.059 0.003 0.033×3 0.069 0.059 0.063
7c -OO^{t}Bu	^{t}BuOOH (1.5 M) / hν in toluene/CH_2Cl_2 (9/1) at 298k	*Trans* [a] R= 0,9987	T_1 (68%) T_2 (32 %) 2×10^7	5.041 4.737	1.216 1.223	1.119 0.995	0.045×3 0.007 0.073 0 0.045×3 0.007 0.073 0.074
	at 223k	Trans [a] R= 0,9988	T_1 (76 %) T_2 (24 %) 0.37×10^7	5.250 4.861	1.224 1.228	1.220 0.724	0.019×3 0.055 0.064 0.076 0.019×3 0.100 0.064 0.076
		Or Trans [b] R= 0,9988	T_1 (77%) T_2 (23 %) 0.64×10^7	5.239 4.925	1.226 1.223	1.244 0.683	0.061×3 0.061×3
7c -OH	Fenton reaction in 0.1 M buffer at 298k	*Trans* (85%) *Cis* (15%)	1 species 1 species	5.343 5.522	1.368 1.397	1.065 1.677	0.026×3 0.063 0.038 0.012 0.047×3 0.083 0.061 0.025
	Nucleophilic addition : H_2O / $FeCl_3$/ O_2 at 298k	*Trans* (66 %) *Cis* (34 %)	1 species 1species	5.345 5.516	1.367 1.399	1.061 1.701	0.056×3 0.056×3 0.085
7c -CH$_3$	Fenton reaction /DMSO 5% /Argon in 0.1 M buffer at 298k	I & II	1 species	5.745	1.491	1.822	0.061×3 0.042 0.033 0.273
7c -CH$_2$OH	Fenton reaction / 10 % MeOH in 0.1 M buffer at 298k	I & II	1 species	5.784	1.446	1.937	0.060×3 0.023 0.042 0.042
7c -CH(OH)Me	Fenton reaction / 10 % EtOH in 0.1 M buffer at 298k	I & II	1 species	5.794	1.446	1.979	0.052×3 0.088 0.068 0.033
7c -COOH	Fenton reaction / 10 % HCOOH in 0.1 M buffer at 298k	*Trans*	1 species	5.440	1.406	1.623	0.049×3 0.025 0.034 0
7c -CH$_2$C(O)H	Fenton reaction / 10 % CH$_3$-CHO in 0.1 M buffer at 298k	I & II	1 species	5.755	1.475	1.877	0.056×3 0.062 0.054 0.031

The regression coefficient R of each simulation is R > 0.983. [a] Classical Simulation; [b] two dimensional simulation..

³E-like
a_P = 4.2- 4.8 mT a_{He} < 1 mT

T₂ of **8**-OOHt   T₁ of **7c**-OO^{t}Bu   T₁ of **6t**-OO^{t}But   **7t**-OHt

< ³E-³T₄ >
a_P = 4.8 - 5.2 mT a_{Hp-e}= 1 - 1.2 mT

T₂ of **7c**-OOHt   T₂ of **7t**-OOHt   T₁ of **6t**-OOHt   T₂ of **7c**-OO^{t}Bu

³T₄
a_P = 5.3-5.6 mT a_{Hp-e} = 1.2 - 1.4 mT
                 a_{Hp-a} = 2 - 2.3 mT

T₁ of **7c**-OOHt   T₂ of **6t**-OO^{t}But   **7c**-OHt

<³T₄ -E₄>
a_P = 5.5 - 6 mT $a_{H p-e / b}$ = 1.4 - 1.8 mT
                 $a_{H p-a / b}$ = 1.7 - 2 mT

7c-COOHt   T₁ of **7t**-OOHt   T₂ of **6t**-OOHt   **7c**-OHc

E₄-like
a_P = 5.7 - 6 mT $a_{H b}$ = 1.6 - 1.9 mT

7c-CH₃ or **7c**-CH₂(OH) or **7c**-CHMe(OH)

⁵T₄
a_P = 5.2 - 4.8 mT $a_{H b}$ = 1.7- 2 mT

8-OHc

⁴T₃
a_P = 3.6 - 4.3 mT $a_{H p-e / b}$ = 1.4- 1.9 mT

T₁ et T₂ of **6t**-OOHc   **7t**-OHc

< ⁴T₃-E₃>
a_P =3.6 - 4.3 mT $a_{H p-e}$ = 1 - 1.4 mT
                 $a_{H p-a}$ = 2 - 2.5 mT

T₁ et T₂ of **7t**-OOHc   **7t**-CH₂(OH)t

Scheme 4 Average geometries of the 5R nitrone adducts in phosphate buffer.

intrinsic flexibility of the 5–membered nitroxide ring can be characterized by the amplitude and phase of the ring deformation. Because of the dihedral rules followed by the β-coupling of the electron of the nitroxide, (see table 2 calculated for DEPMPO-OOH[16]) the major set, in this first simulation solution of the **7c**-OOH$_t$ signal, has the A_p and A_H values characteristic for pseudo-axial phosphoryl group and pseudo-equatorial H of a twist envelope (³T₄ for 2R,4S,5R-nitroxyde or ⁴T₃ for 2S,4R,5R-nitroxyde). Therefore the OOH group is also pseudo-axial and the hydromethyl group is

Table 2 Relation between the geometry of the substituent P or H_β and their coupling constants for DEPMPO adducts[16]

X (H_β or P) position	<XCNPz Dihedral angle (°)	A_P (mT)	$A_{H\beta}$ (mT)
axial	6.5	5.93	2.57
pseudo-axial	17.6	5.45	2.36
Bisectional	30	4.5	1.95
pseudo-equatorial	42.4	3.27	1.41
equatorial	53.5	2.12	0.92

equatorial. The minor set adopts an average geometry with distortion of the twist ring, that is traduced by a C-P bond less

axial (lower A_p value) and a more axial OOH group (lower A_H value). This geometry is named, <³E-³T₄>[17] for the 2R,4S,5R-adduct **7c**-OOH$_t$ (see Scheme 4). In the second simulation solution (with a higher A_p difference for the two sets), the preponderant conformer, with the smallest Ap and aH values, adopts the previously invoked distorted twist geometry towards one envelope geometry (<³E-³T₄> for the 2R,4S,5R-adduct **7c**-OOHt; see Scheme 4), when the geometry of the minor conformer is distorted from the twist to the other envelope geometry, (<³T₄ – E₄> for the 2R,4S,5R- adduct 7c-OOHt ; see Scheme 4). Therefore, in this second simulation solution, one of the groups, either OOH group or the phosphorus one, is less axial when the other is more. Nevertheless, the pseudo-axial positions of the C-P bond or C-OOH bond do not minimize the steric interactions, however, these positions stabilize the adduct by anomeric interactions,[7,18] because of a strong hyperconjugative interaction of the orbitales σ* of the C–P bond or σ* of the C2–O bond with the π or the π∗ of the N-O•. Both solutions show a higher average value for Ap of **7c**-OOHt than that of DEPMPO-OOHt therefore a more axial

position of the phosphorus group inducing a higher anomeric stabilizing effect of the CP bond on the NO$^\bullet$ moiety. This stabilizing interaction explains in part the higher persistency of **7c**-OOHt when compared with DEPMPO-OOHt.

From recent theoretic QM/MM/MD calculations, the noticeable asymmetry of the signal of the DMPO-OOH adduct is proved also to result from a slow chemical exchange between two conformation "families" (or "sites", or "sets"), with a different dihedral angle $\angle OOCN$ and separated by a 7 Kcal/ mol-1 energy barrier.[19] In one family, the OOH group ($\angle OOC2N = 80°$) is above the ring main plane, while in the other family, the OOH group is oriented in the periphery of the ring ($\angle OOC2N$ of 300°). In each family, a fast interconversion occurs between $^3T_4$-like (H$_\beta$ pseudo-equatorial) and $^4T_3$-like (H$_\beta$ pseudo-axial) conformations of the ring. The hfsc coupling constants A_N and $A_{H\beta}$ showed that these two twist geometries are in equivalent populations. Theoretic QM/MM/MD calculations prove also that the rotation around the C_2-O bond in DMPO-OH adduct does not induce a conformational slow exchange, [20] as it can be supposed for DMPO-OOH.

For **7c**-OOHt, we can consider that, as for DMPO, the rotations around the O-O bond, and around the C_2-O bond, contribute to the slow conformational exchange. Furthermore, the presence of the crowding substituents on the aminoxyl ring such as the hydroxymethyl and phosphorus groups can increase the energy barrier between the two conformations $^3T_4$ or $^4T_3$, and

therefore, limits the $^3T_4/^4T_3$ equilibrium. This steric effect can explain an average geometry close to $^3T_4$ for the 2R,4S,5R-adduct and close to $^4T_3$ for the other enantiomer.

In the rest of the text, for the signals obtained with **7t**, **6** and **8** nitrones, we report the solutions of simulation with the highest regression coefficients. From several solutions of simulation, with similar regression coefficients, we selected arbitrarily those with the smallest difference between populations of the conformer sets in chemical exchange. The equality of the populations was also an initial hypothesis to begin the simulation.

The trapping of superoxide with the other diastereoisomer, (4R*,5R*), 4-HM$_{trans}$DEPMPO (**7t**) where the phosphoryl group and the hydroxymethyl substituent are in trans position led to more complicated spectra (fig 1b) owing the formation of two diastereoisomer adducts, but also of some minor nitroxides (around 10%), that could be issued from decomposition of the superoxide adducts. The major signal of the **7t**–OOH spectra, (fig 1b) exhibited a dramatically alternating linewidth (varying from 0.1 mT up to 0.5 mT) with a phosphorus coupling constant smaller than that of the minor signal (see Table 3). Therefore, this signal was simulated with an exchange model of two sets of conformers (with a low exchange rate) and, was attributed to the superoxide adduct **7t**-OOHc, resulting on the cis-addition on the **7t** ring face of the phosphoryl group. Both

Table 3   Esr parameters of some radical adducts with nitrones 4-HMDEPMPO (**7t**) and MEOOPPO (**8**) *a*t 298K.

Adduct	Adduct generating system	Diastereoisomer	Conformers & Exchange rate k (s^{-1})	A_P (mT)	A_N (mT)	$A_{H\beta}$ (mT)	$A_{H\gamma}$ (mT)			
7t-OOH	(HX / O$_2$/ XO) in 0.1 M buffer	*Trans* (32%)	T$_1$ (56 %) T$_2$ (44 %) 0.62×10^7	5.366 5.289	1.248 1.300	1.529 0.923	0.020×3 0.020×3	0.082 0.082	0.059 0.059	0.044 0.044
		Cis (68%)	T$_1$ (70 %) T$_2$ (30 %) 0.02×10^7	4.220 4.247	1.397 1.414	1.301 1.061	0.047×3 0.047×3	0.064 0.064	0.030 0.030	0.025 0.025
7t-OH	Fenton reaction in 0.1 M buffer	*Cis* (76%) *Trans* (24%)	1species 1species	4.277 4.237	1.397 1.401	1.758 0.974	0.045×3 0.045×3	0.045 0.07	0 0	0 0
	Nucleophilic addition :H$_2$O / FeCl$_3$/O$_2$	*Cis* (70%) *Trans* (30%)	1species 1species	4.272 4.228	1.394 1.399	1.754 0.962	0.040×3 0.040×3	0.045 0.070	0 0	0 0
7t-CH$_2$OH	Fenton reaction / 10 % MeOH in 0.1 M buffer	*Cis* (80%) *Trans* (20%)	1species 1species	4.155 3.992	1.471 1.497	1.733 2.480	0.027×3 0.027×3	0.053 0.048	0 0	0 0
8-OOH	(HX / O$_2$/ XO) in 0.1 M buffer	*Trans*	T$_1$ (52 %) T$_2$ (48 %) 0.88×10^7	4.869 5.102	1.303 1.311	0.909 1.001	0.043×3 0.043×3	0.067 0.067	0.027 0.027	0.020 0.020
	KO$_2$ / C$_6$O$_6$H$_{18}$ / DMSO) in 0.1 M buffer	*Trans*	T$_1$ (51 %) T$_2$ (49 %) 0.31×10^7	5.224 4.911	1.301 1.300	1.007 0.796	0.055×3 0.055×3	0.107 0.107	0.028 0.028	0.028 0.028
8-OH	Fenton reaction in 0.1 M buffer	I (60%) II (40%)	1 species 1 species	4.990 5.205	1.378 1.411	0.955 1.678	0.058×3 0.058×3	0.109 0.076	0.039 0.039	0.030 0.030
8-CH$_2$OH	Fenton reaction / 10 % MeOH in 0.1 M buffer	I (94%) II (5%)	1 species	5.379 5.538	1.450 1.462	1.815 2.242	0.049×3 0.049×3	0.071 0.030	0.023 0.023	0.022 0.022
8-CHMeOH	Fenton reaction /10 % EtOH in 0.1 M buffer	I	1species	5.401	1.447	1.791	0.056×3	0.098	0.033	0.028
8-COOH	Fenton reaction / 10 % HCOOH in 0.1 M buffer	I (89%) II (11%)	1 species 1 species	5.393 5.219	1.433 1.433	1.433 2.131	0.020×3 0.020×3	0.034 0.112	0.023 0.023	0.022 0.022

conformer sets of **7t**-OOHc, adopt an average geometry distorted from the twist geometry where the phosphorus group is nearly bisectional for hydroxylmethyl groups pseudo-equatorial, and for C_2-H bond nearly equatorial and therefore, C_2-OOH bond pseudo-axial, ($<^4T_3$-$E_3>$ geometry for the 2S,4R,5R-adduct **7t**-OOHc; see Scheme 4). A minor signal with a higher phosphorus coupling constant was assigned to the trans superoxide adduct **7t**-OOHt. This second signal was also simulated with an exchange model of two conformer sets which adopt an average geometry distorted from the twist geometry because the phosphorus can be more ou less pseudo-axial when the hydroxylmethyl group is axial and C_2-H bond can be equatorial or bisectional ($<^3E$-$^3T_4>$ and $<^3T_4$-$E_4>$ geometry for the two conformers sets of 2R,4R,5R- adduct **7t**-OOHt; see Scheme 4). The positions (pseudo-axial) of the three crowded substituents explain the small ratio of this trans adduct. The conformer exchange rate for **7t**-OOH_c or for **7t**-OOH_t presented a lower value than that of **7c**–OOH_t, traducing an enhanced energy barrier between the conformer set. The slowing down of the exchange rate of the **7t**-OOH_t conformers in comparison with that of **7c**–$OOH_{t,}$ in same ratio, can be explained by vicinity of the hydroxymethyl group towards the hydroperoxyle group that could reduce the OOH free motion around the C_2-O bond or the O-O bond. In the case of the **7t**–OOH_c conformers, the motion of the OOH group can be altered by the steric hindrance of the phosphoryl group.

The bicyclic nitrone MEOOPPO (**8**) was expected to afford only the *trans* superoxide adduct because of the rigid geometry of its pyrroline ring and because one of its faces was overcrowded. The signal observed when using the ([XO / O_2 / HX] generating system was not intense and not persistent; three scans were necessary to obtain a signal (fig 1c) that could be analyse although its fast vanishing. The spectrum of Fig. 1c was better simulated by two species in chemical exchange (see Table 3; correlation coefficient R of simulation is about 0.96 when it is about 0.90 by using only one species) with a C-P bond in between pseudo-axial and bisectional orientation. The two signals were assigned to the *trans* diastereoisomer adduct. The occurrence for this nitrone also of the conformational exchange is a proof that it is due the rotations around the C_2-O bond or the O-O bond. Nevertheless, the average geometries of the two conformer sets in slow exchange looked like more envelopes than twist geometries (^3E for one conformer set and ($<^3E$-$^3T_4>$ for the other set of the 2R,4S,5R- adduct **8**-OOH_t; see Scheme 4) with HOO- group pseudo-axial but -CH_2OH equatorial. This nitroxide had the smallest coupling constants A_P observed for trans adduct in our nitrone series. Therefore, the weak intensity of the signal could be attributed to the degradation of the nitrone itself as to a weak persistency of the

superoxide adduct because of its geometry inducing a too weak stabilization by anomeric or hyperconjugative effects. When using the [KO_2 / crown ether] generating system in the presence of **8**, the observed spectra were more complex because of the superimposition of three signals. One signal was assigned to the superoxide adduct; the second was assigned to one diastereoisomer adduct of the hydroxyl radical, and the third, to one of its degradation species.

The trapping of superoxide with nitrone 3-HMDEPMPO **6** (fig 1d) led also to complicated spectra owing the formation of two diastereoisomer adducts of the diastereoisomer **6t** (94 % of **6**) but also of minor nitroxides (10%) that could be issued from decomposition of the superoxide adducts or from adducts on **6c**. The main signals of the spectra (fig 1d) observed for the 3-HMDEPMPO nitrone were therefore simulated by two pairs of signals (see Table 4). Each pair of signals described the signals of two species in slow chemical exchange. Because the high phosphorus coupling constants, one of these signal pairs could be assigned to the trans adduct **6t**-OOH_t. It appeared in some average geometries distorted from the twist geometry because the OOH or the phosphorus group could be less pseudo-axial when the hydroxylmethyl groups is equatorial ($<^3E$-$^3T_4>$ or $<^3T_4$-$E_4>$ conformations for T_1 or T_2 respectively of the 2R,3S,5R-adduct). The minor signal pear was assigned to the *cis*-adduct **6t**-OOH_c in a twist geometry ($<^4T_3>$ conformations for T_1 and T_2 of the 2S,3S,5R-adduct) with the OOH group pseudo-axial/ bisectional when the hydroxymethyl group is axial and the phosphorus group is pseudo-equatorial. The simulation proved also lower values of the exchange rates between the conformer sets of the *trans* adduct when compared to **7c**–OOH_t conformers, traducing the effect of the C_3 substitution, trans versus the phosphoryl group, and the modification of the neighborhood of the OOH moiety. These results were coherent with the observations done in the case of the analogue nitrone, 3-PhDEPMPO.

(b) Spin Trapping of some peroxyl radicals: Trapping of the methylperoxyl radical in aqueous medium was investigated with 4-HM_{cis}DEPMPO **7c** in a comparison aim of the signal shape of its adduct with that of superoxide adduct. The methylperoxyl radical was generated in aqueous buffer by oxidation of the methyl radical formed by attack of the hydroxyl radical on DMSO. The eight-line signal (major signal in fig 2a) of its adduct with nitrone **7c** showed a strong broadening of the internal lines of each quartet and a high dissymmetry that suggest again the presence of two conformers for one diastereoisomer adduct (*trans*) of this peroxyl radical. It was satisfactorily simulated with this assumption (Table 1) and was found superimposed to traces of the methyl radical adduct.

Table 4 Esr parameters at 298 K of several radical adducts with 3-HMDEPMPO mainly at 298K.

Adduct	Adduct generating system	Diastereoisomer	Conformers & Exchange rate k (s⁻¹)	A_P (mT)	A_N (mT)	$A_{H\beta}$ (mT)	$A_{H\gamma}$ (mT)
6t-OOH	(HX / O₂ / XO) in 0.1 M buffer	*Trans* (64%)	T₁ (68%)	5.027	1.304	0.945	0.020×3 0.069 0.091 0.048
			T₂ (32%)	5.576	1.301	1.426	0.020×3 0.069 0.091 0.048
			1.28×10^7				
		Cis (36%)	T₁ (53%)	3.492	1.379	1.949	0
			T₂ (47%)	3.632	1.314	1.485	0
			4.26×10^7				
	or (KO₂ / C₆O₆H₁₈ / DMSO) in 0.1 M buffer	*Trans* (60%)	T₁ (68%)	5.045	1.302	0.950	0.022×3 0.070 0.087 0.053
			T₂ (41%)	5.557	1.298	1.424	0.022×3 0.070 0.087 0.053
			1.36×10^7				
		Cis (40%)	T₁ (55%)	3.500	1.380	1.932	0
			T₂ (45%)	3.623	1.322	1.502	0
			3.98×10^7				
6t-OO^{t}Bu	^{t}BuOOH (1.5 M) / hv in toluene/CH₂Cl₂ (9/1) At 298 °K	*Trans* (75%) [a]	T₁ (59%)	4.867	1.214	0.767	0.044×5 0.099
			T₂ (41%)	5.261	1.207	1.348	0.044×5 0.103
			1.20×10^7				
		Cis (25%)	T₁ (55%)	3.564	1.270	1.167	0×5 0.070
			T₂ (45%)	3.826	1.249	1.493	0×5 0.111
			2.92×10^7				
	At 223 °K	*Trans* (75%) [b]	T₁ (39%) [c]	5.117	1.203	1.021	0.045×5 0.103
			T₂ (61%) [c]	4.613	1.229	0.474	0.045×5 0.103
			0.05×10^7				
6t-OH	Fenton reaction in 0.1 M buffer	I (86%)	1 species	5.134	1.380	0.848	0.038×3 0.082 0.053 0
		II (14%)	1 species	5.443	1.399	1.778	0.038×3 0.060 0.053 0
	or H₂O / FeCl₃/O₂ [b]	I (53%)	1 species	5.444	1.402	1.826	0.036×3 0.061 0.042 0.033
		II (47%)	1 species	5.105	1.395	0.815	0.036×3 0.082 0.041 0.032
6t-CH₂OH	Fenton reaction / 10 % MeOH in 0.1 M buffer	I (69%)	1 species	5.603	1.452	1.669	0×5 0.059
		II (31%)	1 species	5.403	1.485	0.925	0×5 0.052
6t-COOH	Fenton reaction / 10 % HCOOH in 0.1 M buffer	I (89%)	1 species	5.612	1.444	1.486	0×5 0.059
		II (11%)	1 species	5.191	1.456	0.886	0×5 0.033

The regression coefficient R of each simulation is R > 0.983. [a] *Classical Simulation ;* [b] *two dimensional simulation.*

The conformers sets of adduct **7c**-OOMe adopt similar averaged geometries than the superoxide adduct conformers: a twist geometry for the major conformer set ($^3T_4$ for 2R,4S,5R-nitroxyde) and a twisted distorted-bent average geometry for the minor conformer set ($<^3E$-$^3T_4>$ for the 2R,4S,5R-nitroxyde). However, the C-P bond of **7c**-OOMe was found slightly more bisectional than that of **7c**-OOH.

The trapping of the *tert*-butylperoxl radical in an organic medium such as toluene-dichloromethane (9/1) was investigated as it allowed to study the conformational exchange by varying the temperature and to approach the thermodynamic and kinetic parameters of this exchange at low temperature. This trapping was tested with **7c** and **6** as it offered a new comparison view on the ring substitution effect. A classical simulation with the ROKI program[13] of the signal observed at room temperature was done for each nitrone. This program was also used for a two dimensional simulation (field- temperature) of the whole set of the spectra recorded at various temperatures. The simulation was done by optimizing the set of coupling constants and the thermodynamic parameters such as, the average activation energy between the two conformers, the preexponential factor of the Arrhenius relation, the entropy and enthalpy terms. [21] This simulation method allowed to obtain the coupling constant values of the two conformers, their populations p_i and their exchange period τ_i at the various temperatures and to calculate the value of the exchange rate ($k = p_1 \times 1/\tau_1 + p_2 \times 1/\tau_2$). In tables 1 and 4, the parameters are given at 283°K and, above all, at 223°K, where, due to the slowest exchange (lowest kinetic rate), the most reliable hf constants for the conformational analysis can be obtained. The resulting spectrum with **7c** proved a stereo-selective addition of

the tBuOO• radical and the signal of the resulting trans adduct was also an eight-line signal with a dissymmetry quite similar to that of the **7c**-OOH signal in buffer. The signal of this peroxyl adduct **7c**–OO^{t}Bu$_t$ was studied at various temperature from 223 K to 308 K, (three examples are given in Figure 2b to d). A broadening of the lines and an increase of dissymmetry was observed with decrease of temperature. This reversible change confirmed the model of two conformers for peroxyl-adducts. The major conformer with the larger A$_P$ and A$_H$ values adopts, at any temperatures, a distorted twist-bent average geometry (<^{3}E-^{3}T$_4$> for the 2R,4S,5R-adduct **7c**-OO^{t}Bu$_t$) when the minor conformer adopts the bent average geometry (^{3}E-like for the 2R,4S,5R-adduct) with in both cases a pseudo-axial C$_2$-OOtBu orientation. This orientation can stabilize nitroxide moiety by an anomeric interaction, because of a strong hyperconjugative interaction of the σ*(C$_2$–O) bond with the π (N-O$^•$). If compared with *trans* DEPMPO-OO^{t}Bu adduct,[22] the *cis* C$_4$-substitution by the hydroxymethyl group does not affect the average geometries of the conformers sets nor the exchange rate. The hydroxymethyl group can have an outer-ring orientation minimizing its interaction with the cis phosphoryl group.
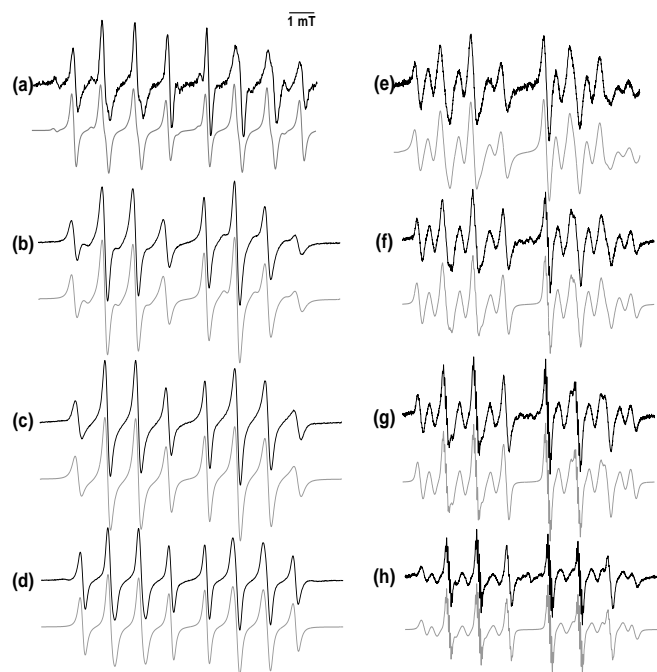

Figure 2. **Spin trapping of peroxyl radicals with nitrones 7c or 6.** Spectrum (dark lines) obtained and simulated (grey lines) from a mixture containing (a) **7c** (10 mM), H$_2$O$_2$ (2 mM), FeSO$_4$ (2 mM), DTPA. (1 mM), DMSO (5 %) in phosphate buffer (0.1 M), pH 7.3 after 1 min incubation under O$_2$ atmosphere. (b) **7c** (20 mM) and ^{t}BuOOH (1.5 M) in deoxygenated toluene/CH$_2$Cl$_2$ (9/1) UV-photolysed at 223 K. (c) as (b) at 258°K. (d) as (b) at 298°K. (e) as (b) but with **6** at 223°K. (f) as (b) but with **6** at 243°K. (g) as (b) but with **6** at 263°K. (h) as (b) but with **6** at 283°K *Spectrometer settings: microwave power, 10 mW; modulation amplitude, 0.497 mT (a), 0.217 mT (b-d),0.124 mT (e-h); time constant, 0.28 ms (a), 0.64 ms (b-h); gain 10^5 (a), 8 × 10^4 (b-d), 5 × 10^4 (e-h); sweep time, 84 s (a),167.77 s (b-d),671 s (e-h) ; conversion time, 82 ms (a), 163.84 ms (b-d),655.36 ms (e-h).*

As for superoxide, the trapping, with **6**, of ^{t}BuOO$^•$ radicals in toluene-dichloromethane (9/1) led to complicated spectra owing the formation of two diastereoisomer adducts of the diastereoisomer **6t** with the preponderance, however, of the *trans* adduct. A temperature study of the signal shape afforded the spectra given in Fig. 2e, 2f , 2g and 2h. The signals of **6t**-OO^{t}Bu (Fig. 2h) exhibited at ambient temperature and even below visible γ$_{AH}$ hyperfine coupling constants that allowed an accurate simulation of both signals (table 4). At the low temperature of 223°K, the signals are broadened and the hyperfine lines disappeared (Fig. 2e).

The major conformer of the trans adduct **6t**-OO^{t}Bu$_t$ (minor at 298°K) adopts a bent geometry (^{3}E for the 2R,3S,5R-adduct) with a strongly equatorial C$_2$-H bond when the second conformer adopts a twist conformation (^{3}T$_4$ for the 2R,3S,5R-adduct). In the bent geometry conformation, the axial orientation of OOtBu makes its steric interaction strong with the pyrroline ring while stabilizing the nitroxyde by an anomeric interaction. While the phosphorous and hydrogen couplings are smaller compared to the values of DEPMPO, the exchange correlation times (not given herein) are very long at 223°K, and therefore, the exchange rate is slowed at this low temperature. The value of the exchange kinetic constant of **6t**-OO^{t}Bu$_t$ is smaller than those calculated for **7c**-OO^{t}Bu.The thermodynamic parameters of the conformational exchange between the ^{t}BuOO$^•$ adducts with **7c** or **6** calculated at 223 K are given in Table 5. The rate of OO^{t}Bu rotation is strongly affected by the pseudo-rotation of pyrroline ring. The energy barrier of this OO^{t}Bu rotation is increased by the substitution at C$_4$ in comparison with DEPMPO-OO^{t}Bu. This is evidenced by the slightly larger E$_a$ or ΔH$^{#2}$ values, but the impact on the entropy ΔS$^#$ is more important and just compensate for **7c** the hindering effect of a larger barrier. Therefore, the ΔG$^#$ free energy of barrier is the same than for DEPMPO-OO^{t}Bu.

The steric interaction is strongly magnified if the pyrroline ring has a substituent on the position 3 with a *cis*-orientation with respect to the OOtBu group. This fact is indicated in the above table by the very large E$_a$ and ΔH$^#$ values of **6**-OO^{t}Bu. Though the ΔG$^#$ free energy of barrier is also increased compared to the non-substituted pyrroline ring at the position 3, the difference is not as large, since the transition state is entropically disfavored (see ΔS$^#$). The reduced entropy difference is caused primarily

Table 5. Thermodynamic parameters at 223 K of the tBuOO• radical adduct of nitrones DEPMPO, **7c** and **6**.

Adduct	DEPMPO- OO^{t}Bu	**7c**-OO^{t}Bu	**6**-OO^{t}Bu
ΔH$_R$^{1,2} in kJ.M^{-1}	0.20	0.64	-2.07
ΔS$_R$^{1,2} in J.K^{-1}M^{-1}	-6.50	-12.71	-5.43
ΔG$_R$^{1,2} in kJ.M^{-1}	1.73	3.15	-0.46
ΔH$^{#2}$ in kJ.M^{-1}	11.41	14.99	26.39
E$_a$^{1} in kJ.M^{-1}	13.50	15.14	27.31
ΔS$^{#2}$ in J.K^{-1}.M^{-1}	-58.11	-44.93	-15.30
ΔG$^{#2}$ in kJ.M^{-1}	28.73	28.38	30.95

[a] Calculated by the Arrhenius plus Van t'Hoff equations
[b] calculated by the Eyring plus Van t'Hoff equations

by the entropy loss of conformers between which the transition takes place. The above observations reveal that the jump of OO^{t}Bu rotamer, from one stable orientation to the other, is almost equally blocked energetically and entropically, but the entropic effect is reduced for substitution both at position 4 and 3, but in the latter case the effect is more important. The two rotamers of of **7c**-OO^{t}Bu have closely identical energy (see the small ΔH_R values), but their populations are more significantly affected by the adaptation of ring geometry to the orientation of OOtBu group (see the variation of ΔS_R). For **7c**-OO^{t}Bu the adaptation is not really efficient (ΔS_R is increased). Interestingly, the two conformers of **6t**-OO^{t}Bu are affected from entropic point of view, in the same amount: the ΔS_R values of adducts DEPMPO-OO^{t}Bu and **6t**-OO^{t}Bu are nearly equal. The broader energetical gap traduced by higher values of the average activation energy between the two conformers sets for **7c**-OO^{t}Bu and particularly for **6**-OO^{t}Bu adducts explained the preponderance of one conformer set when compared with DEPMPO-OO^{t}Bu adduct but also the slower exchange rate at low temperature for **6**-OO^{t}Bu.

(c) Spin Trapping of the hydroxyl radical: The hydroxyl radical was generated in phosphate buffer at pH 7.3 using hydrogen peroxide and ferrous sulphate (Fenton system). Incubation of the nitrones with the hydroxyl radical generating system led to the ESR signals given in Fig. 3. We verified the complete inhibition of signal when catalase was added to the generating mixture. Assignment of some signals in each spectrum recorded for each nitrone to the corresponding hydroxyl adduct was supported by comparison with the signals observed after oxidation (by oxygen) of the hydroxylamines formed by the nucleophilic addition of water on nitrones in the presence of iron III (FeCl^{III} 0.5 mM).

Once again the spectra obtained in Fenton experiments with the *cis* diastereisomer **7c** were more intense and simpler than those obtained with the other nitrones. The solvated hydroxyl radical was expected to attack **7c** on the side opposite to the diethoxyphosphoryl group. The major 12 lines signal in Fig. 3a, had indeed the A_P and A_H values characteristic for pseudo-axial phosphoryl and hydroxyl orientations in a twist structure ($^3T_4$ for 2R,4S,5R-nitroxyde) that could be assigned to the *trans* hydroxyl adduct **7c**-OH$_t$. The more crowded *cis* HO$^\bullet$ adduct **7c**-OH$_c$ led to a minor signal (13 %) with the A_P and A_H values indicating a more axial phosphoryl group for a orientation more bisectional of the C_2-H and therefore a distorted twist geometry to bent geometry ($<^3T_4$-$E_4>$ like structure for 2S,4S,5R-nitroxyde). The signal of this *cis* adduct was superimposed in a higher percentage (30%) to the signal of **7c**-OH$_t$, in the spectrum observed after nucleophilic addition of water on **7c** and subsequent oxidation of the hydroxylamine formed (Fig 3b). In both experiments the signal of the *cis* adduct increased with time of incubation when the signal of *trans* adduct decreased.

7c-OH can be obtained by transformation of the superoxide adduct **7c**-OOH (Fig. 3c) by addition of glutathion peroxydase (GPO) with reduced glutatione (GSH) in the reaction mixture.

In this experiment the *trans* adduct **7c**-OH$_t$ was observed with only a trace of **7c**-OH$_c$ ($< 5\%$). This result confirmed the almost exclusive *trans* addition of superoxide on nitrone **7c**.

Two minor signals were also superimposed to the **7c**-OH signals in the spectrum issued from the Fenton experiment (fig 4a). They were assigned to **A** (11%, $A_N = 1.415$ mT, $A_P = 5.756$ mT, $a_{H\beta} = 1.948$ mT), and **B** (6%, $A_N = 1.516$ mT, $A_P = 6.099$ mT, $a_{H\beta} = 2.298$ mT), two adducts on **7c**. The nitroxide **B** increased to 27% after 1h30 incubation. From their coupling constant values, **A** and **B** appeared carbon centred radical adducts (cf. next paragraph) because of their high $a_{H\beta}$ values denoting pseudoaxial C_2-H. However, **B** was assigned to a *cis* adduct because of tallest A_p and a_H values ($<^3T_4$-$E_4>$) for the 2S,4S,5R-adducts). when **A** was assigned to a *trans* adduct (in E_4-like geometry for the 2R,4S,5R-adducts). **A** and **B** might be issued from the addition on nitrone **7c** of a radical resulting from one hydrogen abstraction on the hydroxylmethyl substituent of a second **7c** molecule (see Scheme 5). The hydrogen bonding between the hydroxyl groups of the two molecules involved can reinforced the *cis*-addition.
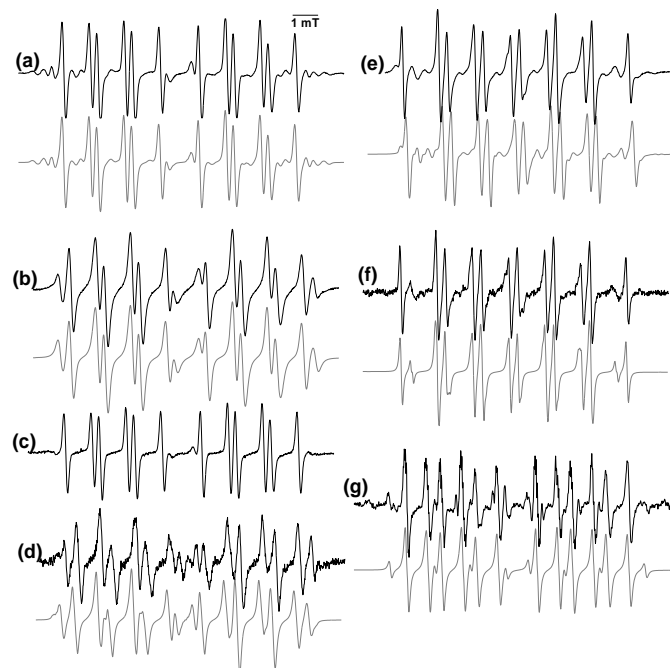

Figure 3. ESR signals of hydroxyl radical adduct with nitrones 7c and 7t, 8 and 6. Spectra obtained (dark lines) and computer simulated (gray lines) after incubation (a) 1 min of **7c** (61 mM) in phosphate buffer 0.1 M, at pH 7.3 containing H$_2$O$_2$ (2 mM), FeSO$_4$ (2 mM), DTPA (1 mM). (b) 10 min of **7c** (20 mM). FeCl^{III} 0.5 mM in pure water. (c) 9 min of **7c** (61 mM) in phosphate buffer 0.1 M at pH 7.3 containing HX (0.4 mM), XO (0.04 U mL^{-1}), DTPA (1 mM), to which then GPO (10 mM) and GSH (1.2 mM) were added. (d) as (a) but with **8** (50 mM). (e) as (a) but with **7t** (50 mM). (f) as (b) but with **7t** (20 mM). (g) as (a) but with **6** (50 mM). *Spectrometers settings: microwave power 10 mW; modulation amplitude, 0.497 (a-f), 1 (g); time constant, 0.128 s; gain 105; sweep time, 83.89 s; conversion time, 82 ms.*
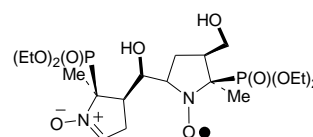
Scheme 5. General chemical structure of A and B.

The spectrum (Fig 3e) observed after incubation of the other diastereoisomer **7t** with hydroxyl radicals showed superimposition of two signals that were both assigned to the hydroxyl adduct in two diastereoisomeric forms (Table 3). The ratio between the two diastereoisomers was almost the same after nucleophilic addition of water in presence of iron III and subsequent oxidation of the hydroxylamine formed (Fig 3f). The major adduct was assigned to the *cis*-adduct **7t**-OHc in a twist average geometry with C_2-H bond in between pseudo – equatorial and bisectional orientation ($<^4T_3->$ for 2S,4R,5R-nitroxyde). The minor *trans* -adduct **7t**-OHt was found in a bent average geometry with axial C_2-H bond and a bisectional C-P bond (^{3}E-like for 2R,4R,5R-nitroxyde).

Incubation of the hydroxyl radical generating system in the presence of the cyclic nitrone MEOOPPO **8** led to a spectrum (Fig 4d) that was satisfactorily simulated assuming the presence of three species. The major signal was assigned to the trans adduct **8**-OHt adduct in a bent average geometry with axial C_2-H bond and a bisectional C-P bond (^{3}E-like for 2R,4S,5R-nitroxyde). The minor *cis* adduct presented a relatively low phosphorus coupling constant in respect to its high hydrogen coupling constant (Table 3). Therefore, this adduct was found in an twist average geometry with a C-P bond more bisectional than pseudo-axial et C_2-H bond more bisectional than pseudo-equatorial (^{5}T4 for 2S,4S,5S-nitroxyde). The third species with C_2-H bond more bisectional was not defined (15%, $A_N = 1.439$ mT, $A_P = 5.191$ mT, $A_{H\beta} = 2.131$ mT). Adducts on **8** of carbon centred species were proved to exhibit an higher phosphorus coupling constant. Because of the relatively fast disappearances of both hydroxyl adducts, this persistent third species was proved to be of another nature.

The nitrone **6** afforded in the presence of hydroxyl radicals a spectrum (Fig 3f) composed with two major signals with very different $a_{H\beta}$ values (Table 4) and closed A_P and A_N and g values assigned to the major *trans* and the minor *cis* OH-adducts on **6t**. Both signals were recorded after the nucleophilic addition of water in the presence of Fe^{III} but in different percentage. They are each in a twist distorted average geometry ($<^3E-^3T_4 >$ for the major signal 2R,3R,5R-adduct **6t**-OH$_t$ and $<^3T_4-E_4>$ for the minor signal assigned to 2S,3R,5R-adduct **6t**-OH$_c$). Another little signal was also involved in each spectrum (15 % for Fenton experiment and 4% for nucleophilic addition; $A_N = 1.45$ mT, $A_P = 5.83$ mT, $A_{H\beta} = 1.44$ mT) resulting probably from the degradation of the first species.

(d) Spin-Trapping of centred radicals: some minor species observed when the hydroxyl radical was generated might be due to the trapping of several carbon centred radicals. Since the hydroxyl radical can easily abstract hydrogen atoms on the α-carbon atom of an alcohol, the reactivity of the hydroxyl radical towards the hydroxymethyl group of the pyrroline ring may be involved. Therefore, we studied the trapping of various carbon centred radicals generated by a hydrogen abstraction on C-1 of alcohol (methanol or ethanol) or acid (HCOOH) or by the

scission of the C-S bond of DMSO (affording the methyl radical). We report, in Fig. 4, the spectra observed after the trapping of these various carbon centred species by **7c**. A residual trace of the trans hydroxyl adduct can be seen sometimes in the spectra. For comparison, the spectrum observed after the prolonged incubation of **7c** in the Fenton experiment showing also the presence of adduct **B** (cited before) was given in Fig. 4a. In the experiments of Fig 4b, c, d, and e, the main signals of the spectrum issued for the carbon centred radical trapping were relatively simple, and at first view can be assigned to only one species although the assymetric internal lines.

We investigated the trapping of carbon centred radicals with the others nitrones and generally two species diastereoisomer were obtained (Table 3 and 4). One example is given with nitrone **7t** in Fig. 4f showing the complexity of the spectrum. The major adduct was assigned again to the *cis* adduct in a twist average geometry with C_2-H bond in between pseudo–equatorial / bisectionnal orientation ($<^4T_3->$ for 2S,4R,5R-nitroxyde). The trans adduct **7t** -CH$_2$OH$_t$ was found in a twist distorted average geometry $<^4T_3-E_3>$ conformation for 2R,4R,5R-nitroxyde).
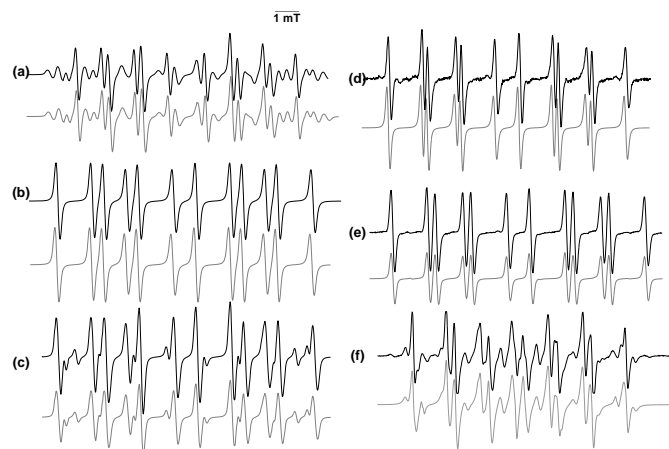

Figure 4. Spin trapping of carbon centred radicals by nitrone 4-HMDEPMPO. Spectra obtained (dark lines) and computer simulated (gray lines) from phosphate buffer (0.1 M, pH 7.3 containing **7c** (61 mM), H_2O_2 (2 mM), $FeSO_4$ (2 mM), DTPA (1 mM) (a) after 1h30 incubation; (b) after 3 min incubation in the presence of MeOH (10%); (c) after 1 min incubation in the presence of EtOH (10%); (d) after 1 min incubation in the presence of HCOOH (10%). (e) after 10 min incubation in the presence of DMSO (5%) under argon atmosphere; (f).as in (b) but in presence of **7t**. *Spectrometers settings: microwave power 10 mW; modulation amplitude, 0.497 (a,b, e), 0.702 (c), 0.01 (d); time constant, 0.128 s; gain 10^5 ; sweep time, 83.89 s; conversion time, 82 ms.*

By submitting alcohol or formiate to the action of the hydroxyl radical, in presence of **6** or **8**, two signals (spectra not shown) were formed presenting close g and a_N values and high A_P values (Tables 2 and 3) that can be explained by an axial or pseudo-axial orientation of the C-P bond. For **8** adducts, the high a_H traduces a pseudo-axial orientations of C_2-H bond of trans adduct and a C_2-H bond bisectional for *cis* adduct. In contrary, the a_H values differs for **6** adducts with a pseudo-equatorial orientation of C_2-H for the *trans*-diastereoisomer in a minor ratio (small a_H value ; $<^3E-^3T_4 >$ for the 2R,3R,5R-adduct

6t-R$_t$) and a major *cis*-adduct with various orientations of the C$_2$-H bond traducing possible hydrogen bonding of the hydroxylmethyl substituent with the group added.

Degradation of the Superoxide adduct

We already shown[9] that the half-life time of **7c**-OOH$_t$ was 21 min when the half-life time of adduct DEPMPO-OOH was 15 min 30s and that the decay of the **7c**-OOH has a predominant first order character. In comparison with the other nitrones of our series, its superoxide adduct is the more persistent. In experiments with both superoxide generating system systems and in spite of argon bubbling the decay of the signal of the superoxide adduct **7c**–OOH was observed with increase of another nitroxide signal that was identified as the hydroxyl adduct. From the simulation of the spectra of Fig. 5a (R= 0.988) and 6b (R= 0.988) we admitted the involvement of 53 % and 14.3 % respectively of the *trans* hydroxyl adduct but also of 8.7% and 5.5 % of the *cis* hydroxyl adduct respectively. The ratio of the *cis* hydroxyl adduct to the *trans* adduct was higher than that observed when the superoxide adduct was transformed into the hydroxyl adduct by the system [GPO / GSH].
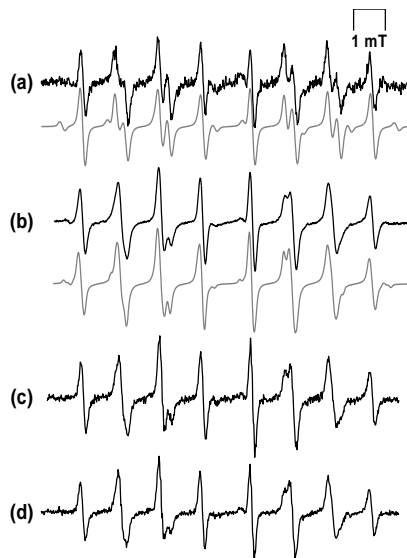

Figure 6. **Evolution of observed (dark lines) and simulated (grey lines) spectra in superoxide trapping with 7c** (a) after 52 min incubation of **7c** (50 mM) in phosphate buffer (0.1 M, pH 7.3 containing KO$_2$ (10 mM) / DMSO (10%). (b) after 1h16 incubation under argon bubbling of **7c** (61 mM) containing HX (0.4 mM), XO (0.04 U mL^{-1}), DTPA (1 mM). (c) after 16 min incubation of **7c** (50 mM) and mannitol (100 mM) in phosphate buffer (0.1 M, pH 7.3) containing KO$_2$ (10 mM) / DMSO (10%). (d) after 16 min incubation of **7c** (50 mM) and catalase (100 U mL^{-1}) in phosphate buffer (0.1 M, pH 7.3) containing KO$_2$ (10 mM) / DMSO (10%). *Spectrometers settings: microwave power 10 mW (a-e); modulation amplitude, 0.313 (a-b), 0.702 (c), 0.22 (d-e); time constant, 1.28 ms (a-e); gain 10^5 (a-e); sweep time, 83.89 s (a-e); conversion time, 82 ms (a-e).*

As the hydroxyl adduct might be observed after a nucleophilic addition of water on nitrone, solutions of nitrone **7c** were let 24h in 100 mM neutral phosphate buffer and without a supplemental addition of metal traces. After an oxygen bubbling, we did not observed ESR signal of **7c**-OH adduct. Therefore, the hydroxyl radical adduct observed in the

superoxide trapping experiments originated from the superoxide adduct decay. Addition of a high concentration of mannitol (6 time higher than the nitrone concentration) (fig 6c) or of catalase (2600 u ×mL^{-1}, fig 6d) inhibit the *cis* hydroxyl adduct formation but did not inhibit the *trans* hydroxyl adduct (18 % and 23% after 16 min incubation respectively) indicating that the *trans* hydroxyl adduct was directly produced from the superoxide adduct. However, formation of the *cis* hydroxyl adduct in the absence of mannitol proved the production of the hydroxyl radicals in the degradation pathway. Furthermore the hydroxyl adduct appeared faster with increasing KO$_2$ concentration. Slower degradation of the superoxide adduct and slower apparition of the hydroxyl adduct were observed when using (XO/ O$_2$ /HX) generating system instead of KO$_2$ system (fig 7b) and the argon bubbling has a supplementary beneficial effect. Therefore the oxidant species such as superoxide and hydrogen peroxide are probably involved in this degradation mechanism. Thus this degradation into the hydroxyl adduct is not spontaneous and should not occur *in vivo* in a preponderant manner at the biological concentration encountered in oxidant species.

Experimental

Chemicals

Drying of the solvents was made by distillation under inert atmosphere in the presence of sodium and benzophenone for THF, diethyloxide and toluene, in the presence of magnesium for methanol, ethanol and P$_2$O$_5$ for dichloromethane. Melting points were taken on a B510 Büchi capillary apparatus and were left uncorrected. ^{31}P NMR, ^{1}H NMR and ^{13}C NMR spectra were recorded at 121.49, 300.13 and 75.54 MHz respectively, or at 81.01, 200.13 and 50.32 MHz respectively. ^{31}P NMR was taken in CDCl$_3$ using 85% H$_3$PO$_4$ as an external standard with broad-band ^{1}H decoupling. ^{1}H NMR and ^{13}C NMR were taken in CDCl$_3$ using TMS or CDCl$_3$ as internal reference, respectively. Chemical shifts (δ) are reported in ppm and coupling constant *J* values in Hertz. The assignments of NMR signals were facilitated by use of the DEPT 135 sequence for all products. Interpretation of some spectra was achieved by comparing ^{1}H homonuclear correlation (NOESY ^{1}H-^{1}H). Positive ion ES mass spectra and tandem mass spectra were acquired in a triple quadripole mass spectrometer equipped with a pneumatically assisted ES source (nebulizing gas, AIR at a 0.8 L/min).

Ethyl 2-cyano-4-diethoxypentanoate (2). The mixture of ethyl 2-cyano-4-oxopentanoate **1** [12] (10.0 g, 59.2 mmol) and resin Amberlyst 15 (4.5 g) in triethylorthoformate (45 mL) was stirred for 20 h at 0-5 °C. After resin filtration and extraction with CH$_2$Cl$_2$ (10 mL) the solvent and triethylorthoformate were evaporated under reduced pressure to afford pure ethyl 2-cyano-4-diethoxypentanoate **2** as a green oil (14.2 g, 99% yield). ^{1}H NMR (100.13 MHz) δ 4.26 (2H, q, *J* = 7.2), 3.6 (1H, m), 3.47 (2H, q, *J* = 7.0), 3.44 (2H, q, *J* = 7.0), 2.2-2.4 (2H, m),

1.4 (3H, s), 1.33 (3H, t, J = 7.1), 1.17 (3H, t, J = 7.1), 1.16 (3H, t, J = 7.1). ^{13}C NMR (40.5 MHz) δ 167.1 (s), 117.9 (s), 100.2 (s), 63.0 (s), 56.6 (s), 56.5 (s), 37.8 (s), 33.8 (s), 22.4 (s), 15.5 (s), 14.1 (s).

2-Aminomethyl-4-diethoxypentanol (3) At a solution of LiAlH$_4$ (4.3 g, 113.1 mmol) in THF (70 mL) was added dropwise at 20-30 °C a solution of **2** (14.9 g, 61.3 mmol) in THF (130 mL). Then the mixture was stirred for 3 h at 25 °C and 1 h at 57 °C. The reaction mixture was next treated by addition of brine (100 mL) saturated with NaCl and extraction with Et$_2$O (3 × 200 mL). The organic layer was dried over Na$_2$SO$_4$ and after evaporation of the solvents the residue was distillated under reduced pressure (95-100 °C/0.05 mmHg) to give rise to pure 2-aminomethyl-4-diethoxypentanol as a white oil (4.5 g, 36% yield not optimized). ^{1}H NMR (100.13 MHz) δ 3.65-3.75 (2H, m), 3.51 (2H, q, J = 7.2), 3.47 (2H, q, J = 7.2), 2.84 (1H, m), 2.5-2.6 (2H, m), 1.8-1.9 (1H, m), 1.55-1.65 (2H, m), 1.36 (3H, s), 1.16 (3H, t, J = 7.2).

Diethyl (4-hydroxymethyl-1-methylpyrrolidin-2-yl) phosphonate (5). The solution of **3** (2.9 g, 19.02 mmol) in THF/H$_2$O (5:1, 72 mL) was stirred for 3 h in the presence of 5% HCl. It was next stirred for 2 h at pH 8 after addition of K$_2$CO$_3$. After saturation with NaCl of the solvents the product was extracted with Et$_2$O (3 × 25 mL). The organic layer was dried over Na$_2$SO$_4$ and after evaporation of the solvents, the residue was verified as 4-hydroxymethyl-1-methyl-2-pyrroline **4** through ^{13}C NMR (25.1 MHz, C$_6$D$_6$) δ 175.3, 64.3, 63.5, 42.0, 39.6, 19.3. This residue was then stirred for 7 days at 25 °C in the presence of diethylphosphite (2.7 g, 19.4 mmol). After that, water (30 mL) was added and the mixture was acidified until pH 1. The aqueous layer was washed with CHCl$_3$ (4 × 15 mL) then basified with K$_2$CO$_3$ and extracted with CHCl$_3$ (4 × 15 mL). The resulting organic layer was dried over Na$_2$SO$_4$ and evaporation of the solvents under reduced pressure lead to a brown oil corresponding to **5** (1.9 g, 40% yield) in mainly (1R*, 4R*) configuration. ^{31}P NMR (25.1 MHz) δ 29.48 (3%); 29.0 (97%); ^{1}H NMR (100.13 MHz) δ 4.15 (4H, five lines, J = 7.0, 7.0), 3.5-3.7 (3H, m), 3.1-3.3 (1H, m), 2.8-3.0 (1H, m), 2.1-2.3 (4H, m), 1.4 (3H, d, J = 13.0), 1.32 (6H, t, J = 7.0); ^{13}C NMR (40.5 MHz) δ 65.0 (s), 62.3 (s), 62.0 (s), 59.9 (C^{IV}, d, J = 161.3), 49.5 (d, J = 5.5), 42.1 (d, J = 3.5), 37.7 (d, J = 3.2), 24.3 (d, J = 6.8), 19.3 (s), 16.5 (s),.

5-Diethoxyphosphoryl-3-hydroxymethyl-5-methyl-1-pyrroline N-oxide (6). Phosphonate **5** (1.76 g, 6.63 mmol) was added to sodium tungstate (0.097 g, 29.4 mmol) dissolved in 3 mL of distilled water and 6 mL of methanol. To the solution cooled down to 0 °C, 30% H$_2$O$_2$ (1.43 mL, 0.378 mol) was added dropwise. The pale yellow reaction mixture was stirred at 0 °C until the colour darkened, then it was stirred at 4 °C for 48 h. When the reaction was virtually complete the aqueous layer was saturated with NaCl and the expected nitrone was extracted with CH$_2$Cl$_2$ (4 × 10 mL). The collected organic phase was dried over Na$_2$SO$_4$ and the solvent was removed under reduced pressure. The crude nitrone was purified with chromatography on silicagel eluting with CH$_2$Cl$_2$/EtOH (86:14) and this allowed

us to collect pyrroline N-oxide **6** (0.6 g, 32% yield) in mainly (3R*, 5R*) configuration as a yellow oil. ^{31}P NMR (25.1 MHz) δ 22.15 (3%); 21.8 (97%); ^{1}H NMR (100.13 MHz) δ 7.06 (1H, q, J = 2.8, 2.8), 4.91 (1H, s,), 4.0-4.5 (4H, m), 3.2-3.8 (3H, m), 2.6-3.1 (1H, m), 1.8-2.2 (1H, m), 1.7 (3H, d, J = 15.0), 1.35 (6H, t, J = 7.0). ^{13}C NMR (40.5 MHz) δ 139.5 (d, J = 8.3), 74.8 (C^{IV}, d, J = 154.2), 63.9 (d, J = 6.5), 62.9 (d, J = 7.5), 62.0 (d, J = 4.5), 42.1 (s), 33.3 (s), 21.0 (s), 16.4 (s), 16.1 (s). C$_{12}$H$_{24}$NO$_8$P requires: C 45.28; H 7.60; N 5.28. Found: C 45.0; H 7.81; N 5.15.

(6-Ethoxy-6a-methyl-5-oxa-6-oxophospholan-6-yl)-1-pyrroline-N-oxide (MEOOPPO) (8). To a solution of nitrone **7c** [9] (0.2 g, 0.75 mmol) in (4R*,5R*) configuration in dimethoxyethane (5mL) was added oily NaH (60%, 0,017 g, 0.045 mmol) at 0 °C. The reaction mixture was stirred for 16 h at room temperature. The precipitate was filtered and washed with CH$_2$Cl$_2$ (10 mL). The mixed filtrates were concentrated under reduced pressure to give the crude product. It was purified by flash chromatography on silicagel eluting with CH$_2$Cl$_2$/EtOH (85:15) to afford the pure nitrone **8** as a red oil in 45% yield (0.075 g, 0.34 mmol). ^{31}P NMR (121.49 MHz) δ 34.07; ^{1}H NMR (300.13 MHz) δ 6.81 (1H, q, J = 2.5), 4.5-4.03 (4H, m), 3.20-2.90 (2H, m), 2.70-2.53 (1H, m), 1.84 (3H, d, J = 14.9), 1.35 (3H, t, J = 7.0); ^{13}C NMR (75.47 MHz) δ 131.7 (d, J = 7.7), 74.5 (C^{IV}, d, J = 131.1), 67.0 (d, J = 8.8), 66.0 (d, J = 7.5), 45.6 (d, J = 11.0), 31.5 (s), 19.5 (d, J = 3.3), 16.3 (d, J = 6.6). ESI-MS/MS (20 eV) m/z (%): 220.2 (100) [M + H]$^+$, 192 (26), 174 (3), 156 (25), 138 (2), 110 (14), 94.1 (20).

Spin Trapping Studies.

Xanthine oxidase (XO), bovine erythrocyte superoxide dismutase (SOD) and catalase were purchased from Boehringer Mannheim Biochemical Co.; diethylenetriaminepentaacetic acid (DTPA) and other chemicals were purchased from Sigma Chemical Co. ESR spectra were recorded at room temperature using a Bruker ESP 300 ESR spectrometer at 9.5 GHz (X-band) employing 100 kHz field modulation. Reaction mixtures were prepared in a chelex-treated phosphate buffer (0.1 M, pH 7.3).

Superoxide trapping with hypoxanthine-xanthine oxidase generating system. XO (0.04 U mL^{-1}) was added to a mixture of nitrone (50 to 60 mM), DTPA (1 mM), and HX (0.4 U mL^{-1}) in phosphate buffer (0.1 M, pH 7.3). When SOD (606 U mL^{-1}) was added to the HX/XO generating system for an inhibition test of superoxide trapping, it was added before XO addition.

Superoxide trapping using KO$_2$/18-crown-6 generating system. ESR signal observed upon incubating the reaction mixture obtained after adding KO$_2$ (10 mM final concentration) and 18-crown-6 ether (10 mM final concentration) in DMSO to phosphate buffer (0.1M, pH 7.3) containing nitrone (50 to 60 mM final concentration).

Hydroxyl trapping using Fenton generating system. The hydroxyl radical was generated by addition of FeSO$_4$ (2 mM) to a mixture of nitrone (50 to 60 mM), DTPA (1 mM), and H$_2$O$_2$ (2 mM) in phosphate buffer (0.1 M, pH 7.3). When catalase

(600 U mL^{-1}) was added to the incubation mixture for an inhibition test of hydroxyl trapping, it was added before FeSO$_4$ addition.

(HO)H$_2$C$^\bullet$ Trapping: The carbon centred of MeOH was generated by the Fenton system in the presence of nitrone (61 mM) and MeOH (10%).

H$_3$C-(OH)HC$^\bullet$ Trapping. The carbon centred of EtOH was generated by the Fenton system in the presence of nitrone (61 mM) and EtOH (10%).

HOOC$^\bullet$ Trapping. The carbon centred of HCOOH was generated by the Fenton system in the presence of nitrone (61 mM) and HCOOH (10%).

Methyl Trapping. The methyl radical adduct was generated by Fenton System in the presence of nitrone (61 mM) and DMSO (5%) under argon atmosphere.

Conclusion

In the series of pyrroline *N*-oxide with a phosphonate group, the dynamic process between two rotamers of superoxide or peroxyl adducts appeared difficult to avoid. Between the hydroxymethyl substituted analogues of DEPMPO, the *cis* isomer C$_4$ substituted 4-HMcDEPMPO is the only one to trapped superoxide and peroxyl radicals in a stereoselective manner. The presence of a hydroxylmethyl group on the C$_4$ of the pyrroline ring in the *cis* position favors addition of the superoxide radical on the face opposite to the phosphoryl group. The ESR signal of the superoxide or peroxyl adduct of 4-HMcDEPMPO were more easily assignable than for DEPMPO: the alternating line-width phenomenon due to the chemical exchange between the conformer sets is existing (0.1 mT up to 0.25 mT) but less visible. In comparison with DEPMPO (k = 15,7 × 10^7 *for DEPMPO-OOH,*[14] k = *0.9 × 10^7* at 223 k for DEPMPO-OO^{t}Bu), the presence of a hydroxylmethyl group on the C$_4$ of the pyrroline ring on the face of the phosphoryl group slows down the pseudo-rotation of the rotamers of the *trans* superoxide adduct (9 fold smaller exchange rate) and slightly that of the *trans* terbutylperoxyl-adduct. (2 fold smaller exchange rate at 223°K). The conformational exchange broadening slightly the lines of the signal did not impede the reading of the corresponding spectra. The shapes of the signals of the 4-HMcDEPMPO-OOHt and 4-HMcDEPMPO-OORt adduct are strongly characteristic of the species added and can be easily recognized in spectra with superimposed signals of adducts of various kinds of radicals. For conformers of both superoxide adduct and methylperoxyl radical adduct, the pseudo-axial C-OOH bond (and also the C-P bond for the major conformer) can stabilize the nitroxide moiety by anomeric effects. Moreover this axial position of the C-P bond of the 4HMcDEPMPO-OOHt can explain its persistency 25% higher than the one of DEPMPO-OOH. Despite C$_4$ substitution does not limit the dismutation of the nitroxide, as a possible alternative reaction path, the major

decay mechanisms observed in our buffer experiment involved some concentration of oxidant that can be modulate. Therefore, this nitrone appeared as a very good tool for superoxide or peroxyl radicals detection. The substitution on the C$_4$ of the pyrroline ring on the opposite face to the phosphoryl group slows down the pseudo-rotation of the rotamers of the *trans* superoxide adduct (25 fold smaller exchange rate) but the spectra are more complex because of a non stereoselective addition of superoxide and a weaker persistency of the adduct. When the conformation of the ring substituted in C$_4$ position was blocked by a second cycle involving phosphonate, the bicycle formed was too much constrained and did not afford a superoxide adduct particularly persistent because of a pseudo-equatorial orientation of the C-P bond. In comparison with DEPMPO the presence of a hydroxylmethyl group on the C$_3$ of the pyrroline ring on the face opposite to the phosphoryl group slows down the pseudo-rotation of the rotamers of the *trans* superoxide adduct (12 fold smaller exchange rate) and particularly of the *trans* terbutylperoxyl-adduct. (18 fold smaller exchange rate at 223°K) but it does not impede it wholly. Moreover in these substitution case, superoxide and peroxyl diastereoisomer adducts were obtained; their superimposed ESR signals afforded complex spectra. Every nitrone studied presented two diastereoisomer adducts with hydroxyl radical, although, the *cis* addition with the *cis* isomer C$_4$-substituted 4-HMcDEPMPO was also disfavored. With carbon centred radicals diastereoisomer adducts were also generally obtained, exept for nitrone 4HMcDEPMPO.

Acknowledgements

Notes and references

1 B. Halliwell, *Am. J. Med.*, 1991, **91**, 3C, 14S; B. Halliwell and J. M. C. Gutteridge, *Am. J. Med.,* 1984, **219**, 1; B. Halliwell and S. Chirico, *Am. J. Clin. Nutr.*, 1993, **57(S),** 715S.

2 a) E. Finkelstein, G. M. Rosen and E. J. Rauckman, *J. Am. Chem. Soc.*, 1980, **102**, 4994. b) A Samuni, C. Murali Krishna, P. Riesz, E. Finkelstein and A. Russo, *Free Radicals Biol. Med*, 1989, **6**, 141. c) G. R. Buettner, *Free Rad. Res. Comms.*, 1990, **10**, 11.

3 a) C. Frejaville, H. Karoui, B. Tuccio, F. Le Moigne, M. Culcasi, S. Pietri, R. Lauricella and P. Tordo, *J. Med. Chem.,* 1995, **38**, 258. b) S. Barbati, J. L. Clément, G. Olive, V. Roubaud, B. Tuccio and P. Tordo, *Free Radicals in Biology;* Environment, Ed. F. Minisci, NATO ASI Series, Life Sciences, Kluwer Academic Publishers : Dordrecht (Netherl;s), 1997, **chapter 3**, 39.

4 H. Karoui, F. Chalier, J.- P. Finet and P. Tordo, Org. Biomol. Chem., 2011, **9**, 2473.

5 J. C. Matasyoh, P. Schuler, H. B. Stegmann, J. L. Poyer, M. West and E. G. Janzen, *Magn. Res. Chem*., 1996, **34**, 351-359.

6 L. Dembkowski, J.-P. Finet, C. Frejaville, F. Le Moigne, R. Maurin, A. Mercier, P. Pages, P. -L. Stipa and P. Tordo, *Free Rad. Res. Com.*,

1993, **19**, S23. C. Chachaty, C. Mathieu, A. Mercier and P. Tordo, *Magn. Res. Chem.*, 1998, **36**, 46.

7 C. Nsanzumuhire, J.-L. Clément, O. Ouari, H. Karoui, J.-P. Finet and P. Tordo, *Tetrahedron Lett.*, 2004, **45**, 6385.

8 M. Hardy, F. Chalier, J.-P. Finet, A. Rockenbauer and P. Tordo, *J .Org. Chem.*, 2005, **70**, 2135

9 F. Chalier.; M. Hardy, J.-P. Finet, O. Ouari, A. Rockenbauer and P. Tordo, *J .Org. Chem.*, 2007, **72**, 7888.

10 a) J. W. Davies, J. R Malpass and M. P. J. Walker, *Chem. Soc. Comm.*, 1985, 686. b) M.Pirrung, *Tetrahedron Lett.*, 1980, **21**, 4577. c) P. Hughes, M. Martin and J. Clardy, *Tetrahedron Lett*. 1980, **21**, 4579.

11 a) J. Davoll, *J. Chem. Soc.* 1960, 131. b) F. Seela and U. Lüpke, Chem. Ber. 1977, **110**, 1462.

12 A. Y. Sizov, L. A. Yanovskaya, V. Dombrovskii and A. Baccat *Bull. Acad. SCI. USSR, div. Chem. Sci*. (Engl. Transl) EN 1990, **39**, 2.2, 410 (*Izv. Akad. Nauk, SSSR Ser. Khim.* 1990, 473.

13 A. Rockenbauer and L Korecz,. *Appl. Magn. Reson.* 1996, **10**, 29-43.

14 A. Rockenbauer, J.-L. Clément, M. Culcasi, A. Mercier, P. Tordo and S. Pietri, *J. Phys. Chem. A* , 2007, **111**, 4950.

15 D. Cremer and J. Pople, *J. Am. Cem. Soc.,* 1975, **97**, 1354. *Ibid*, 1358.

16 A. Rockenbauer, L Korecz and K. Hideg, *J. Chem. Soc., Perkin Trans. 2.*, 1993, **11**, 2149. A. Rockenbauer, M. Györ, H. O. Hankovsky and K. Hideg, *ESR study of the conformation of 5- and 6-membered cyclic nitroxides (aminoxyl) radicals. In Electron Spin Resonance;* Symons, M. C. R., Ed.; Royal Society of Chemistry: Cambridge, UK, 1988; **11A**, 145.

17 It was sometimes named <^{3}E-E$_4$> geometry in others papers such as ref. 14.

18 J.-L. Clément, N. Ferré, D. Siri, H. Karoui, A. Rockenbauer and P. Tordo, *J. Org.Chem.,* 2005*,* **70,** 1198.

19 C. Houriez, N. Ferré, D. Siri, P. Tordo, and M. Masella *J. Chem. Phys.,* 2010, **114**, 11793.

20 C. Houriez, N. Ferré, D. Siri, P. Tordo, and M. Masella *J Theor. Chem. Acc.*, 2012, **131**, 1.

21 For a detailed explanation of this simulation method, used also to study the superoxide adduct of DEPMPO, see ref. 14

22 The trans-adduct DEPMPO-OO^{t}Bu adduct T_1 has the parameters: A_N = 1.234 mT , A_P = 5.280 mT, $a_{H\beta}$ = 1.103 mT and T_2 : A_N = 1.234 mT , A_P = 4.798 mT, $A_{H\beta}$ = 0.768 mT with k = *0.9 × 10^7* at 223 k. The cis DEPMPO-OO^{t}Bu adduct was also involved in the spectra signals and the ESR parameters of its two conformers were found to be at 223 k: for T_1 , A_N = 1.333 mT , A_P = 4.075 mT, $A_{H\beta}$ = 0.930 mT and for T_2 : A_N = 1.338 mT , A_P = 3.478 mT, $A_{H\beta}$ = 0.850 mT with k = *2.3 × 10^7*.